HHS Public Access

Author manuscript

Neuroimage. Author manuscript; available in PMC 2016 October 01.

Published in final edited form as:

Neuroimage. 2015 October 1; 119: 33–43. doi:10.1016/j.neuroimage.2015.06.055.

Development of the human fetal hippocampal formation during early second trimester

Xinting Ge[a,b], **Yonggang Shi**[b], **Junning Li**[b], **Zhonghe Zhang**[a,c], **Xiangtao Lin**[a,d], **Jinfeng Zhan**[a], **Haitao Ge**[a], **Junhai Xu**[a], **Qiaowen Yu**[a,c], **Yuan Leng**[a], **Gaojun Teng**[e], **Lei Feng**[a], **Haiwei Meng**[a], **Yuchun Tang**[a], **Fengchao Zang**[e], **Arthur W. Toga**[b,*], and **Shuwei Liu**[a,**]

[a]Research Center for Sectional and Imaging Anatomy, Shandong Provincial Key Laboratory of Mental Disorders, Shandong University School of Medicine, 44 Wen-hua Xi Road, 250012 Jinan, Shandong, China

[b]Laboratory of Neuroimaging, Institute of Neuroimaging and Informatics, Keck School of Medicine of University of Southern California, Los Angeles, CA 90033, USA

[c]Department of Medical Imaging, Provincial Hospital Affiliated to Shandong University, 250021 Jinan, Shandong, China

[d]Department of MRI, Shandong Institute for Medical Imaging, 250021 Jinan, Shandong, China

[e]Department of Radiology, Zhong Da Hospital, Southeast University School of Clinical Medicine, 210009 Nanjing, Jiangsu, China

Abstract

Development of the fetal hippocampal formation has been difficult to fully describe because of rapid changes in its shape during the fetal period. The aims of this study were to: (1) segment the fetal hippocampal formation using 7.0 T MR images from 41 specimens with gestational ages ranging from 14 to 22 weeks and (2) reveal the developmental course of the fetal hippocampal formation using volume and shape analyses. Differences in hemispheric volume were observed, with the right hippocampi being larger than the left. Absolute volume changes showed a linear increase, while relative volume changes demonstrated an inverted-U shape trend during this period. Together these exhibited a variable developmental rate among different regions of the fetal brain. Different sub-regional growth of the fetal hippocampal formation was specifically observed using shape analysis. The fetal hippocampal formation possessed a prominent medial–lateral bidirectional shape growth pattern during its rotation process. Our results provide additional insight into 3D hippocampal morphology in the assessment of fetal brain development and can be used as a reference for future hippocampal studies.

Keywords

High resolution MRI; Fetal brain development; Hippocampal formation; Shape analysis

*Corresponding author. toga@loni.usc.edu (A.W. Toga). **Corresponding author. Fax: +86 531 88382502. liusw@sdu.edu.cn (S. Liu).

Introduction

The hippocampal formation (HF), a critical brain structure in the limbic system, is involved in cognition, learning and memory functions (Hassabis et al., 2007; Yanike et al., 2004; Zaidel, 1995; Bohbot et al., 2000; Arleo and Gerstner, 2000; Bird et al., 2010; Cimadevilla et al., 2014). Abnormalities in HF have been associated with congenital cerebral malformations such as lissencephaly, holoprosencephaly and agenesis of the corpus callosum (Baker and Barkovich, 1992; Atlas et al., 1986), as well as neurological and neuropsychiatric disorders including epilepsy (Bernasconi et al., 2005; Gamss et al., 2009), depression (Tae et al., 2011), Alzheimer's disease (Thompson et al., 2004), Parkinson's disease (Ibarretxe-Bilbao et al., 2008) and schizophrenia (Schobel et al., 2009).

Development of the human fetal HF is a subject of increasing interest as hippocampal injury or deviation of the HF from its normal development trajectory may be a contributor to the neurodevelopmental burden of affected individuals (Sizonenko et al., 2006; Abernethy et al., 2002; Jacob et al., 2011). The human HF comprises a considerable number of complex substructures, including the dentate gyrus, the Cornu Ammonis, the subiculum, and the associated white matter tracts, such as the fimbria and the alveus (Naidich et al., 1987a; Insausti et al., 2010; Amaral, 1999; Bronen, 1992). It is therefore difficult to observe small volumetric or shape changes and changes that occur within the substructure because of the limited resolution of the images obtained with 1.5 T or 3.0 T MR in vivo. In addition, in utero MRI is susceptible to frequent fetal movement and pulsatile motion from maternal arteries.

The hippocampal primordium firstly arises at the dorsal part of the lamina terminalis and can be identified histologically as early as in the 9th GW (Humphrey, 1967; Rakic and Yakovlev, 1968). The HF then undergoes a progressive rotation, as well as many other critical changes in the second trimester (Kier et al., 1997; Insausti et al., 2010; Adamsbaum, 2001; Prayer et al., 2006). The dentate gyrus and Cornu Ammonis progressively fold into the temporal lobe, together with the gradually closing hippocampal sulcus (hippocampal fissure) (Kier et al., 1997; Insausti et al., 2010). By 18 to 20 GW, the fetal HF begins to resemble the adult HF (Kier et al., 1997). However, to date there are no quantitative studies on fetal hippocampal development, especially on the sub-regional changes during its rotational process. Hemispheric or gender differences of the fetal HF during this period also are not well understood.

With the help of high-resolution MRI and postmortem specimens, it is feasible to conduct quantitative studies using volume and shape analyses on the human fetal HF to reveal its developmental course directly. Volumetric studies of the HF have been performed in adult populations and progressively in neonates and fetuses (Jacob et al., 2011; Pruessner et al., 2000; Thompson et al., 2008, 2009). A linear trajectory of hippocampal volume increase was found in healthy fetuses (Jacob et al., 2011) and preterm and full-term infants were found to have larger right hippocampi (Thompson et al., 2009). Shape analysis, on the other hand, has the potential of identifying local surface changes or developmental states of brain (sub) regions, such as hippocampi (Thompson et al., 2004; Tae et al., 2011). Deformation-based or voxel-based morphometric analysis of brain structure has provided new

information previously unavailable using only conventional volumetric measurements (Joseph et al., 2014; Wright et al., 1995; Gerig et al., 2001).

In this study, we aimed to observe the development of the human HF using 7.0 T high-resolution MR images of fetal specimens ex vivo. We analyzed volumetric changes as well as performed shape analysis using our novel surface mapping tools with intrinsic geometry and metric optimization (Shi et al., 2014). Hemispheric differences and the developmental course of the fetal HF were measured. Our results provide useful information concerning the interpretation of MRI signals and the developmental changes of the fetal HF visualized in vitro. The observed growth patterns may improve our understanding and classification of hippocampal abnormalities, which can be used as reference for future hippocampal studies.

Materials and methods

Specimen

41 human fetuses (13 males and 28 females) with a gestational age (GA) of 14 to 22 weeks, which were partially used to study brain development characteristics at the 20th gestational week (GW), subcortical brain structures, cortical folding, and the fetal brain template in previous publications (Zhang et al., 2010, 2011; Meng et al., 2012; Zhan et al., 2013), were included in the study. All fetuses were collected in hospitals of Shandong Province, China. 24 specimens were obtained after medically indicated abortions caused by fetal chromosomal abnormality, teratogenesis infection, stressful intrauterine conditions, or unknown reasons of malformation outside of the brain (such as incurable heart, renal malformations, or osseous dysplasia). 17 specimens were obtained after spontaneous abortions attributed to pregnancy-induced hypertension syndrome, severe uterine traumas caused by accident, too thin endometrium, uterine myoma (Türtscher et al., 1999), or incompetence of internal orifice of the uterus. We also ensured that the maternal pregnancy records were absent of a documented history of excessive alcohol intake, smoking, and severe under-nutrition (Bergsjø and Villar, 1997), as well as seizures in the case of eclampsia (Villar and Bergsjg, 1997). 3.0 T MR pre-scanning was conducted to ensure that the developmental status of the brain structures (such as the cerebrum, cerebral cortex, lateral ventricle, and corpus callosum) was anatomically normal. The GA of the fetuses was determined by the crown-rump length, head circumference, and foot length and/or pregnancy records and was expressed in weeks from the last menstrual period (Guihard-Costa et al., 2002). The specimens were immersed in 10% formalin for preservation without extracting the brain. This study was conducted on the basis of approval from the Internal Review Board of the Ethical Committee at the School of Medicine, Shandong University. Written consent was obtained from the parents after explaining the purpose of the study.

Demographic information of the fetal specimens is listed in Table 1.

MRI data acquisition

All fetuses were scanned with a 7.0 T Micro-MR scanner with a maximum gradient of 360 mT (70/16 PharmaScan, Bruker Biospin GmbH, Germany) in Department of Radiology, Zhong Da Hospital, Southeast University School of Clinical Medicine (Jiangsu Provincial

Key Laboratory of Molecular and Functional Imaging). A rat body coil with an inner diameter of 60 mm was chosen and the axial 2D T2-weighted slice images were acquired with the following parameters: slice thickness, 0.5 mm with no gap; field of view (FOV), 4.0 × 4.0 cm/5.0 × 5.0 cm/6.0 × 6.0 cm; matrix, 256 × 256; TR/TE, 12,000/50 ms; and NEX, 4. The time interval between the collection of specimens and scanning was within two months.

Segmentation protocol of the fetal hippocampal formation

The adult HF was considered to be comprised of the dentate gyrus, the hippocampus (Cornu Ammonis), the subiculum, the small subsplenial, supracallosal, and paraterminal gyri, and the associated white matter tracts — the alveus, the fimbria, and the fornix (Naidich et al., 1987a). Others also defined the HF as comprised of a variety of cytoarchitectonic fields including the dentate gyrus, the hippocampus (Cornu Ammonis), the subiculum, presubiculum, and parasubiculum and the entorhinal cortex (Amaral, 1999; Insausti et al., 2010). In consideration of the fetal MR imaging and prior studies (Amaral and Insausti, 1990; Naidich et al., 1987a, 1987b; Adamsbaum, 2001; Jacob et al., 2011; Müller and O'Rahilly, 1994), as well as the study 'Hippocampal and Limbic Terminology' (Bronen, 1992), the term'Hippocampal formation' was defined to include the dentate gyrus, the Cornu Ammonis, the subiculum, the fimbria and the alveus in this study. We also use the term 'Cornu Ammonis' to replace the above 'Hippocampus' to avoid confusion in nomenclature.

Segmentation of the HF was performed manually using Amira software, which can read the native DICOM imaging data directly and show the 3D results within the segmentation. The left HF was always segmented before the right. The anatomical borders used for segmentation of the HF were based on prior studies (Kier et al., 1997; Amaral, 1999; Naidich et al., 1987a, 1987b; Malykhin et al., 2007; Watson et al., 1992; Jacob et al., 2011) and the 'Atlas of Human Central Nervous System Development' (Bayer and Altman, 2004, 2005) and were traced from the anterior head to the posterior tail using both axial and sagittal planes. Note that although the HF in this paper was comprised of the dentate gyrus (DG), Cornu Ammonis (CA), fimbria, alveus, and subiculum, these structures were indistinguishable (or partly distinguishable) by fetal MR imaging and thus were roughly sampled as a whole complex.

Hippocampal head

In the axial plane, medial border of the hippocampal head is defined by the ambient cistern, while the lateral border is demarcated by the cerebrospinal fluid of the temporal horn of the lateral ventricle (Fig. 1A). The amygdala and hippocampal head are separated by the cerebrospinal fluid of the uncal recess of the temporal horn of the lateral ventricle (Watson et al., 1992; Jacob et al., 2011), which is more clear in the sagittal plane (Figs. 2A, B). The inferior border of the hippocampal head is demarcated by the gray/white matter junction in the axial plane (Jacob et al., 2011). The subiculum, facing the dentate gyrus over the hippocampal fissure, is not prominent in head sections.

In the sagittal plane, the amygdala is clearly seen and adjacent to the hippocampal head by the cerebrospinal fluid of the uncal recess of the temporal horn of the lateral ventricle (Figs.

2A and B). The posterior border of the hippocampal head in the section that passes through the brainstem is the cerebral peduncle and ambient cistern (Fig. 2B).

Hippocampal body

The most inferior section of the hippocampal body is the first section where the uncal recess cannot be seen in the axial plane (Malykhin et al., 2007; Pruessner et al., 2000) and its borders are similar to those used for the head of the HF (Jacob et al., 2011). The hippocampal fissure is also clearly seen in these sections. Differently, the superior border of the body is determined by the adjacent germinal matrix, which lies in the roof and lateral wall of the temporal horn and is a special structure in the fetal brain (Fig. 1B). The alveus that overlies the Cornu Ammonis and the contiguous fimbria are clearly seen in the axial plane and both composed in the body segmentation. The subiculum is prominently characterized by its thick superficial medullary lamina (SML) and lies along the medial and superior curvature of the parahippocampal gyrus (Naidich et al., 1987a; Fig. 1B). It comprises the parasubiculum, presubiculum, and subiculum, and the prosubiculum and overlaps with the border of the Cornu Ammonis. In our paper, the subiculum is simply segmented to include the most medial portion of the SML (as far as to the ambient cistern) because of its undiscerned subdivisions with MR imaging (Naidich et al., 1987a; Fig. 1B).

Hippocampal tail

The most inferior section of the hippocampal tail is the first section where the fornix can be seen in full profile in the axial plane (Malykhin et al., 2007; Pruessner et al., 2000) and its borders are similar to those used for the body (Jacob et al., 2011). Differently, the superior border becomes the fornix and the medial border is the thalamus (Fig. 1C).

In the sagittal plane, the hippocampal tail first appears in the paramedian section that passes through the splenium of the corpus callosum, and presents a wedge of gray matter in the angle between the splenium of the corpus callosum and the isthmus of the cingulate gyrus (Naidich et al., 1987b; Fig. 2C). The hippocampal fissure is clearly observed between the fasciolar/dentate gyrus and retrosplenial cortex. In general, the fasciolar and dentate gyri lie above the hippocampal fissure and merge superiously with the indusium griseum behind the splenium of the corpus callosum. They are hard to distinguish using fetal MRI and are both composed in hippocampal segmentation (labeled DG in Fig. 2C) (Naidich et al., 1987b). The fornix, in this section, lies far away from the hippocampal tail.

Lateral to the splenium section, the posterior margin of the hippocampal fissure becomes the subiculum while the anterior margin is still the dentate gyrus (Fig. 2B). The parahippocampal gyrus and the isthmus of the cingulate gyrus are separated by the anterior calcarine sulcus (ACS). The fornix is well seen in this section and lies anterior to the hippocampal tail.

More laterally, the straight hippocampal fissure has been a line between the subiculum and the dentate gyrus (Fig. 2A). The fimbria presents more clearly and the lateral border of the hippocampal formation becomes the cerebrospinal fluid of the temporal horn as turning medially.

Some brains may have one or two transition sections where the borders of the HF were difficult to identify. In these cases it was necessary to navigate one section forward or backward from this transition section to compare the shape and position of the structures where the borders were clear, and to extrapolate these borders onto the difficult section.

To assess the reliability of this segmentation protocol, ten of the scans were selected randomly two months later and re-segmented. Intra-rater consistency between the two segmentations was calculated using Dice's coefficient:

$$d=\frac{2a}{b+c}$$

where *a* is the number of voxels in both the initial and re-tested segmentation, and *b* and *c* are the number of voxels solely in the initial and re-tested segmentation, respectively. The higher the *d* values, the more reliable our segmentation.

Volume analysis

Prior to volumetric analyses, the intracranial volumes (ICVs) of all subjects were measured manually.

The 41 postmortem fetal specimens of 14 to 22 GW in this study were partially used to build a spatial–temporal template described in our previous publication (Zhan et al., 2013). Acquisition of the ICV was performed using BrainSuite similar to Zhan's methodology.

Binary masks of hippocampi generated from the segmented volumes of each brain and the ICVs were used to compute the absolute and relative ($V_{relative} = V_{absolute} / ICV$) volumes of the HF, respectively.

Shape analysis

The binary masks representing the 3D shapes of the HF were subsequently used to reconstruct surface meshes via outlier detection and boundary deformation (Shi et al., 2010). The localized spurious features caused by manual segmentation were automatically detected using the metric distortion during the Laplace–Beltrami (LB) eigen-projection and were fed to a well-composed and topology-preserving deformation. This process was iterated and the final surface, which had the correct topology and provided accurate and smooth representation of the boundary geometry, was generated (Shi et al., 2010). It was constructed of triangular elements that contain the vertices and faces of the binary mask, which represented the true geometry of the HF (Fig. 3). The number of vertices and faces varied with the size and shape of the HF.

To perform shape analysis, one randomly selected surface mesh was re-meshed to have 1000 uniformly distributed vertices. It was used as the template and then projected onto the rest of the surfaces via an intrinsic surface mapping in the high dimensional LB embedding space (Shi et al., 2014). A conformal map between surfaces with highly uniform metric distortion and the ability of aligning salient geometric features was generated directly by minimizing the distance measure in the embedding space with metric optimization (Shi et

al., 2014). All surfaces were represented with the same triangulation and one-to-one correspondence across vertices. To quantify the growth rate of the local HF, a thickness measure at each vertex of the mapped surfaces was computed as the distance from the corresponding vertex to the medial core of the HF was defined (Shi et al., 2009). Distance fields thus indexed local expansions and contractions in HF surface morphology, and were used for statistical analysis at equivalent HF surface points in 3D.

Statistical analysis

The paired T test was used to examine the volume differences between the left and right hippocampi. Absolute and relative volume trends with increasing gestational age were calculated.

To compute the sub-regional development of the fetal HF, linear regression analysis was performed on the corresponding thicknesses with increasing gestational age. Significance was set to $p < 0.05$.

Results

Segmentation reliability

Our segmentation provided high intra-rater reliability with the average Dice's coefficients for the left and right hippocampi 0.9648 and 0.9692, respectively.

Volume analysis

T test showed that the volume of the right HF was larger than the left ($t(40) = 5.813$, $p < 0.05$).

As shown in Figs. 4A and B, the absolute volumes of both the left and right hippocampi increased almost linearly with increased gestational age. However, the rate of increase decreased after about 18 GW.

As shown in Figs. 4C and D, the relative volumes of both the left and right hippocampi exhibited an inverted-U shape trajectory. The rates of increase went up slowly from GW14 to 17. From GW17 to 22, we observed that the relative volume decreased while the absolute volume still increased. This curve implicated that the HF grew slightly faster than the other brain regions from 14 GW to 17 GW, but more slowly than the other brain regions after that time.

Shape analysis

The mean shape of the HF in both hemispheres computed from the set of registered surface images is shown in Figs. 5 and 6. The regression coefficients that represent the growth rate of the sub-regional HF and p-values calculated from linear regression of the corresponding thicknesses were plotted on the mean shapes.

Thickness increased significantly throughout almost the whole left HF. The degree of increase for superior and inferior regions of the hippocampal body was lower than the other regions. Part of the hippocampal head adjacent to the amygdala (AG), the medial part of the

hippocampal body (approximate subiculum), and the posterior part of the hippocampal tail adjacent to the splenium of the corpus callosum also had a lower rate of increase. The anterior part of the hippocampal head, and the medial (approximate dentate gyrus) and lateral regions of the whole HF, on the other hand, increased faster than the other regions.

Fig. 5 shows the p-value map and regression coefficient map of the left HF.

Thickness increased significantly throughout almost the whole right HF. The rates of increase for superior and inferior regions of the hippocampal head and body, and medial regions of the hippocampal body were lower than the other regions. Part of the hippocampal head adjacent to the amygdala and the posterior part of the hippocampal tail adjacent to the splenium of the corpus callosum also had a lower rate of increase. In contrast, the anterior and most medial parts of the hippocampal head and the lateral regions of the whole HF increased faster than the other regions.

Fig. 6 shows the p-value map and regression coefficient map of the right HF.

Both the left and right HF showed differential sub-regional growth. Except for the region adjacent to the amygdala, the hippocampal head and lateral and medial parts of the total HF grew faster than the inferior and superior parts. Fetal hippocampi possessed a prominent medial– lateral bidirectional shape growth pattern.

Discussion

We conducted quantitative research about human fetal hippocampal development. Rightward volumetric asymmetry was found as early as in the second trimester. Absolute volume of the fetal HF showed a linear trajectory while relative volume tendencies showed an inverted-U shape, which suggested that the fetal HF grew steadily and faster than the other brain regions in the early gestational stages during the time from 14 GW to 22 GW. In the later gestational stages of this period, the fetal HF grew more slowly than the other brain regions. Shape analysis, on the other hand, demonstrated a medial–lateral bidirectional growth pattern of the fetal HF.

Hippocampal development

Hippocampal development is critical to many cognitive functions and several studies have been reported in the recent years. Thompson et al., 2009 found rightward asymmetry with no gender difference in full-term and preterm neonatal hippocampal volumes. Furthermore, Jacob et al., 2011 observed the fetal hippocampal development during the period of 21.3 GW to 31.9 GW using volume analysis and found a linear increase in total hippocampal volume with no hemispheric or gender difference. However, there are no prior volumetric or shape studies of fetal hippocampal development during the period in which the HF is known to rotate (10 GW to 24 GW). In addition, the segmentation in the aforementioned studies was limited by the tissue contrast of the in vivo MRI, which was one of the reasons why hemispheric and gender analyses have been difficult.

Kier et al., 1997 succeeded in identifying changes of the HF in the fetal period (13 GW to 24 GW) and viewed the rotation process using MRI, dissections, and histologic sections of

specimens. However, only 6, 5, and 2 specimens were qualified to acquire MR images, useful dissections, and histologic sections, respectively, which made the observation discontinuous and inadequate for volumetric analysis. Bajic et al., 2012 observed the development of the hippocampal sulcus using postmortem and in vivo MRI (17 GW to 36 GW). Asymmetry was observed, with the right HF developing faster than the left. However, the image quality and resolution were insufficient for volumetric analysis.

In comparison, postmortem specimens are advantageous for acquiring high quality images using high-field strength magnets, reduced slice thickness, smaller field of view and increased acquisition time, which are sufficient for quantitative analysis (Bajic et al., 2012; Zhan et al., 2013; Huang et al., 2006, 2009).

Segmentation protocol

Determination of hippocampal boundaries has been a long-standing debate in neuroscientific and neurological domains. It is also the basis for volume or shape analysis and hard to determine for the fetal HF (Watson et al., 1992; Chakeres et al., 2005; Pruessner et al., 2000; Malykhin et al., 2007). We utilized Watson's, Naidich's, Amaral and Insausti's and Jacob's research and the ‘Atlas of Human Central Nervous System Development’ as references but with some modifications. While delineation of the hippocampal head from the amygdala was difficult in the adult brain (Pruessner et al., 2000; Malykhin et al., 2007; Watson et al., 1992), it was easier in the fetal brain, since the two structures were separated laterally by the uncal recess of the lateral ventricle in the sagittal plane (Fig. 2B). For younger fetuses, the hippocampal head was not completely embedded in the temporal lobe (Kier et al., 1995, 1997, Fig. 7), making the hippocampal head look smaller, however, the borders were nearly the same as those of the older specimens (Fig. 7).

Subiculum segmentation of the hippocampal body was problematic, as the presubiculum, the parasubiculum and the entorhinal cortex of the parahippocampus could not be distinguished clearly. The entorhinal cortex is the anterior portion of the classically defined parahippocampal gyrus and the parasubiculum ends at approximately the same level as the entorhinal cortex. Amaral and Insausti in the book ‘The Human Nervous System’ used thionin-stained brain sections to observe the adult HF (Amaral and Insausti, 1990). Only subtle changes in the cytoarchitectonic characteristics of the presubiculum, the parasubiculum and the entorhinal cortex can be identified. Therefore, the subiculum in this paper is simply segmented to include the most medial portion of the SML (ambient cistern) because of its undiscerned subdivisions with MR imaging. A fraction of the presubiculum was included in the subiculum segmentation.

As to the hippocampal tail, Jacob et al., 2011 chose to terminate the posteriomedial extent of hippocampal tail segmentation on the sagittal plane when the hippocampal head disappeared. Part of the hippocampal tail was excluded in the total hippocampal volume segmentation, which was not accurate enough for volumetric analysis. In our study, we can clearly see the hippocampal fissure between the fasciolar/dentate gyrus and retrosplenial cortex in the para-median section that passes through the splenium of the corpus callosum on the 7.0 T images (Naidich et al., 1987b, Fig. 2C). The hippocampal tail was clearly identified between the splenium of the corpus callosum and the isthmus of the cingulate

gyrus. A fraction of the splenium of the corpus callosum was included in the hippocampal tail segmentation due to the fact that the indusium griseum, which was the dorsal surface of the splenium of the corpus callosum, was a remnant of the previous hippocampal formation (Kier et al., 1995) and was difficult to distinguish from the hippocampal tail.

Hemispheric difference

Hemispheric asymmetries were noted in our study, with the right HF being larger than the left. This is consistent with previous pediatric studies, which found larger right hippocampal volumes as early as term (Pfluger et al., 1999; Utsunomiya et al., 1999). The same result was also seen in preterm and neonatal studies (Thompson et al., 2009). Prior findings showed that hemispheric differences were common in human brains beginning in utero (Bajic et al., 2012), while our results showed that the hippocampal volume asymmetry was present as early as the second trimester. It is known that verbal memory deficits are associated with damage to the left HF, whereas deficits in nonverbal memory are associated with damage to the right HF (Zaidel, 1995). Our results suggest that hippocampal asymmetry can be detected as early as in the second trimester, possibly an early sign of functional differences. Other studies have failed to identify significant differences in the left and right hippocampal volumes from 21.3 GW to 31.9 GW (Jacob et al., 2011). This may be due to lower contrast of the in utero MRI images used in their study, resulting in less accurate segmentation. Another possibility is that the population in their study is different from ours. Hemispheric differences were not significant in the early gestational stages in our study ($t(11) = 2.18$, $p = 0.0519$, 14–17 GWs), compared to the later period ($t(28) = 5.5692$, $p = 5.8681e{-}06$, 18–22 GWs). This may be either due to inaccurate segmentation of the fetal HF during early GWs because it is unclear, even with 7.0 T MRI or there may not be hemispheric differences in the early stage.

Volume analysis

Volume analysis showed the overall development of the fetal HF. Linear and inverted-U shape tendencies of the absolute and relative hippocampal volume development were observed in our research, respectively.

Absolute volume development

From Kier's study, the development of the fetal HF was complex during the time from 13 GW to 24 GW (Kier et al., 1997). The rotation process began at about 14–15 GW and finished at about 18–20 GW; the overall hippocampal structure then resembled that of the adult. By the 24thGW, the HF was already relatively smaller in size in comparison to the parahippocampal gyrus, indicating that the growth of the HF was slowing. In our research, the absolute HF volume grew steadily during the early second trimester and then slowed, which was consistent with Kier's findings. On a similar note, Jacob et al. (2011) found a linear increase in total hippocampal volume from 21.3 GW to 31.9 GW. The nearly linear volume increase in our results is consistent with his finding.

Relative volume development

The human cerebral cortex has three types of architecture: archicortex, paleocortex, and neocortex. The HF belongs to archicortex and develops earlier than the paleocortical and neocortical regions. In addition, the hippocampal formation is the main part of the limbic system, often called the 'visceral brain' and subserves olfaction and visceral activities. It is fitting that the hippocampal formation may develop earlier than the other brain regions.

In another study by Kier, the hippocampal formation was the main structure visible on the medial surface of the cerebral hemisphere at 13 GW, prior to the formation of the corpus callosum (Kier et al., 1995). At 16 GW, the cingulate gyrus, parahippocampal gyrus and corpus callosum began to grow while the HF underwent the rotation process. The subcallosal area, cingulate gyrus, and parahippocampal gyrus and other temporal lobe neocortical areas were more prominent after 18 GW when the rotation of the HF was nearly complete. Rakic also found that the hippocampal primordium arose at the dorsal part of the lamina terminalis and preceded the appearance of the definitive fornix, corpus callosum, and hippocampal commissure (Rakic and Yakovlev, 1968). The hippocampal formation may develop earlier than the other regions within or closely related to the limbic system.

Together with the inverted-U shape tendencies of the relative volume development in our study, it is fitting that the fetal HF grew faster than the other brain regions from 14 GW to 17 GW, but more slowly than the other brain regions after that time.

Shape analysis

The second trimester is considered to be a very active neurogenesis and neuronal migration period in which minor disruptions of fetal brain (sub)regions may vitally affect its development (Miranda, 2012). Shape analysis, as confirmed by prior studies (Tae et al., 2011; Joseph et al., 2014; Habas et al., 2012), is especially suitable for representing regional alterations of critical structures such as the HF and may have the potential for monitoring normal or abnormal sub-regional hippocampal development during this period. In this study, we performed surface reconstruction via Laplace–Beltrami eigen-projection and boundary deformation and used thickness measurements during the shape registration for statistical analysis (Shi et al., 2014). This method is intrinsic enough as positioning changes of the fetal HF have no effect on the statistical results (Fig. 7). Varying developments of fetal hippocampal sub-regions were found at the anterior medial part of the hippocampal head (adjacent to amygdala) and posterior part of hippocampal tail (adjacent to splenium of the corpus callosum), which grew more slowly than the other regions. At the same time, the whole fetal HF showed distinct positioning changes from 14 GW to 22 GW (Fig. 7). The whole HF is becoming horizontal as the hippocampal head folds into the temporal lobe, which is consistent with Kier's study (Kier et al., 1997). As mentioned in Rakic's study (Rakic and Yakovlev, 1968), the rotation and enfolding into the temporal lobe of the hippocampal formation were the results of the growth of the surrounding brain structures such as the corpus callosum, amygdala, and thalamus. Our results confirmed his conclusion.

Additionally, we found that the medial and lateral parts of both the left and right hippocampi grew faster than the superior and inferior parts, which meant that the total HF had a medial–

lateral bidirectional growth pattern. It was similar to Bajic's study (Bajic et al., 2012) which found that the shape of the fully inverted HF was classified as oval with a horizontal long axis. Occurrence of this growth pattern may be due to the closure of the hippocampal fissure, as well as the inconsistent growth rate of different hippocampal sub-regions during the second trimester. Moreover, Moser and Moser (1998) found that different portions of the HF in the longitudinal axis had different functional roles, indicating the human HF was functionally heterogeneous. In summary, different sub-regional growth of the fetal hippocampal formation observed in our study is compatible with earlier work and may be linked to functional differentiation.

Limitations

Our sample size was insufficient for gender statistics by gestational week, unfortunately. Gender differences of the adult HF have been confirmed in many studies (Geuze et al., 2005; Gur et al., 2002; Giedd et al., 1997), while prenatal, neonatal, and fetal hippocampal studies found no gender differences (Thompson et al., 2009; Jacob et al., 2011). One reason may be that the gender differences emerge postpartum.

Fetal specimens with medically indicated abortions attributed to fetal chromosomal abnormality, teratogenesis infection, or stressful intrauterine conditions were included in this study. Teratogenesis infection such as genito-urinary infection may increase the neonatal death rate (Patrick, 1967), while stressful intrauterine conditions such as polyhydramnios was associated with adverse pregnancy outcomes and the risk of perinatal mortality (Sandlin et al., 2013). However, samples with the aforementioned disorders that may injure the fetal brain structures had been excluded (Waldorf and McAdams, 2013). Fetal chromosomal abnormality, on the other hand, may cause significant congenital anomalies and mental retardation in infant, if the pregnancy continues to term (Gaboon et al., 2015). However, 3.0 T MR pre-scanning had been conducted by pediatric neuro-radiologist to ensure that the developmental status of the brain structures, such as the size of the cerebrum, developmental status of cerebral cortex, lateral ventricle, and corpus callosum, was anatomically normal. Several samples (4 in our research) with chromosomal abnormality just have minor effects on the statistical results, even if we cannot find the tiny morphological differences with MR pre-scanning. At the same time, the maternal pregnancy records of the included specimens were all absent of a documented history of excessive alcohol intake, smoking, and severe under-nutrition, as well as seizures in the case of eclampsia, the same inclusion criteria with our previous publications (Zhang et al., 2010, 2011; Meng et al., 2012; Zhan et al., 2013). Additionally, we need note that collection of fetal materials is an extremely difficult work, especially for those with normal brain structures. It is hard to cover all of the gestational weeks during the period from 14 GW to 22 GW if specimens with medically indicated abortions were excluded.

A possible limitation associated with applying this postmortem study to in vivo clinical observation is that one must be cautious to account for morphological differences between the formalin-fixed brain and living samples. Tissue degradation during formalin fixation is frequent in postmortem studies (Yushkevich et al., 2009; Stan et al., 2006; Chakeres et al., 2005; Zhang et al., 2011). Nevertheless, MRI scanning in this work was performed with the

brain in the skull and the time interval between the collection of the fetal specimen and MRI scanning was less than two months. Slight tissue degradation has a minor effect on the volume or shape statistical results. On the other hand, although the present results cannot be used directly in a clinical setting, they provide certain information that is beneficial for evaluating the fetal hippocampal development and interpreting MRI examinations performed at lower field strengths (Lin et al., 2011). Clinical application of measurements obtained on the basis of postmortem brain tissues has been reported by previous studies (Torkildsen, 1934; Zhang et al., 2010; Takahashi et al., 2011).

The lack of histological sections of the developing fetal HF was another limitation of this work. Such fetal material is extremely difficult to obtain and to date no perfect histological section has been available. On the other hand, respective gold standard segmentation of the fetal HF is also unavailable, especially for subfield segmentation. The parasubiculum, the presubiculum and the entorhinal cortex and subfield of the fetal HF are difficult to precisely distinguish using fetal MR imaging data. Nevertheless, our segmentation was performed on the bases of adult and fetal hippocampal studies (Amaral, 1999; Watson et al., 1992; Jacob et al., 2011) and hippocampal atlases (Winterburn et al., 2013; Chakeres et al., 2005; Yushkevich et al., 2009), as well as anatomical studies (Kier et al., 1997; Naidich et al., 1987a, 1987b; Bayer and Altman, 2005; Bayer and Altman, 2004) of fetal and adult HF. We created consistent hippocampal segmentation protocol and got high intra-rater reliability in this study. It is feasible to roughly segment the fetal HF with the help of 7.0 T MR images. Actually, subfield segmentation of the fetal HF is challenging even with histological sections (Amaral and Insausti, 1990). Identification of the brain structures by themselves may not be sufficient for border delineation. Histological samples as references are needed to improve segmentation accuracy in our future work.

Conclusions

This study charted the developmental process of human fetal hippocampal formation during the early second trimester. Asymmetric volume differences of the fetal HF and variable growth among regions of the fetal brain and sub-regions of the fetal HF were exhibited. The human fetal HF develops earlier than the other brain regions and possesses a prominent medial–lateral bidirectional shape growth pattern.

Acknowledgments

We thank the Research Center for Sectional and Imaging Anatomy at Shandong University for fetal specimen collection and the Laboratory of Neuro Imaging Resource (LONIR) at the University of Southern California (USC) for instrument access and technical support. This study was supported by the National Natural Science Foundation of China (no. 31071050; no. 81001223; no. 81301280; no. 81300497; no. 81371533), in part by Doctoral Foundation of Shandong Province (no. 2011BSE27084; no. BS2012YY009; no. BS2013YY025); Specialized Research Fund for the Doctoral Program of Higher Education of China (no: 20120131130008; no: 20120131120043) and National Institutes of Health (NIH) under grant K01EB013633 and grant P41EB015922. Additional research supported was provided by the National Institute of Biomedical Imaging And Bioengineering of the National Institutes of Health under award number U54EB020406.

References

Abernethy LJ, Palaniappan M, Cooke RW. Quantitative magnetic resonance imaging of the brain in survivors of very low birth weight. Arch. Dis. Child. 2002; 87:279–283. [PubMed: 12243993]

Adamsbaum, C. Elsevier Masson; 2001. Atlas d'IRM du cerveau foetal: guide d'interprétation des aspects normaux.

Amaral DG. Introduction: what is where in the medial temporal lobe? Hippocampus. 1999; 9:1–6. [PubMed: 10088895]

Amaral, DG.; Insausti, R. The hippocampal formation. In: Paxinos, G., editor. The Human Nervous System. San Diego: Academic Press; 1990. p. 711-755.

Arleo A, Gerstner W. Spatial cognition and neuro-mimetic navigation: a model of hippocampal place cell activity. Biol. Cybern. 2000; 83:287–299. [PubMed: 11007302]

Atlas SW, Zimmerman RA, Bilaniuk LT, Rorke L, Hackney DB, Goldberg HI, Grossman RI. Corpus callosum and limbic system: neuroanatomic MR evaluation of developmental anomalies. Radiology. 1986; 160:355–362. [PubMed: 3726113]

Bajic D, Canto Moreira N, Wikstrom J, Raininko R. Asymmetric development of the hippocampal region is common: a fetal MR imaging study. AJNR Am. J. Neuroradiol. 2012; 33:513–518. [PubMed: 22116115]

Baker LL, Barkovich AJ. The large temporal horn: MR analysis in developmental brain anomalies versus hydrocephalus. AJNR Am. J. Neuroradiol. 1992; 13:115–122. [PubMed: 1595428]

Bayer, SA.; Altman, J. Atlas of Human Central Nervous System Development: The Human Brain During the Third Trimester. CRC Press Llc.; 2004.

Bayer, SA.; Altman, J. The Human Brain During the Second Trimester. Boca Raton, FL: CRC Press; 2005.

Bergsjø P, Villar J. Scientific basis for the content of routine antenatal care. Acta Obstet. Gynecol. Scand. 1997; 76:15–25. [PubMed: 9033239]

Bernasconi N, Kinay D, Andermann F, Antel S, Bernasconi A. Analysis of shape and positioning of the hippocampal formation: an MRI study in patients with partial epilepsy and healthy controls. Brain. 2005; 128:2442–2452. [PubMed: 16014649]

Bird CM, Capponi C, King JA, Doeller CF, Burgess N. Establishing the boundaries: the hippocampal contribution to imagining scenes. J. Neurosci. 2010; 30:11688–11695. [PubMed: 20810889]

Bohbot VD, Allen JJ, Nadel L. Memory deficits characterized by patterns of lesions to the hippocampus and parahippocampal cortex. Ann. N. Y. Acad. Sci. 2000; 911:355–368. [PubMed: 10911885]

Bronen RA. Hippocampal and limbic terminology. Am. J. Neuroradiol. 1992; 13:943–945. [PubMed: 1590195]

Chakeres DW, Whitaker CD, Dashner RA, Scharre DW, Beversdorf DQ, Raychaudhury A, Schmalbrock P. High-resolution 8 Tesla imaging of the formalin-fixed normal human hippocampus. Clin. Anat. 2005; 18:88–91. [PubMed: 15696533]

Cimadevilla JM, Lizana JR, Roldan MD, Canovas R, Rodriguez E. Spatial memory alterations in children with epilepsy of genetic origin or unknown cause. Epileptic Disord. 2014; 16:203–207. [PubMed: 24913814]

Gaboon NE, Mohamed AR, Elsayed SM, Zaki OK, Elsayed MA. Structural chromosomal abnormalities in couples with recurrent abortion in Egypt. Turk. J. Med. Sci. 2015; 45:208–213. [PubMed: 25790554]

Gamss RP, Slasky SE, Bello JA, Miller TS, Shinnar S. Prevalence of hippocampal malrotation in a population without seizures. AJNR Am. J. Neuroradiol. 2009; 30:1571–1573. [PubMed: 19541778]

Gerig, G.; Styner, M.; Shenton, ME.; Lieberman, JA. Medical Image Computing and Computer-assisted Intervention—MICCAI 2001. Springer; 2001. Shape versus size: improved understanding of the morphology of brain structures; p. 24-32.

Geuze E, Vermetten E, Bremner JD. MR-based in vivo hippocampal volumetrics: 1. Review of methodologies currently employed. Mol. Psychiatry. 2005; 10:147–159. [PubMed: 15340353]

Giedd JN, Castellanos FX, Rajapakse JC, Vaituzis AC, Rapoport JL. Sexual dimorphism of the developing human brain. Prog. Neuro-Psychopharmacol. Biol. Psychiatry. 1997; 21:1185–1201.

Guihard-Costa AM, Menez F, Delezoide AL. Organ weights in human fetuses after formalin fixation: standards by gestational age and body weight. Pediatr. Dev. Pathol. 2002; 5:559–578. [PubMed: 12399830]

Gur RC, Gunning-Dixon F, Bilker WB, Gur RE. Sex differences in temporolimbic and frontal brain volumes of healthy adults. Cereb. Cortex. 2002; 12:998–1003. [PubMed: 12183399]

Habas PA, Scott JA, Roosta A, Rajagopalan V, Kim K, Rousseau F, Barkovich AJ, Glenn OA, Studholme C. Early folding patterns and asymmetries of the normal human brain detected from in utero MRI. Cereb. Cortex. 2012; 22:13–25. [PubMed: 21571694]

Hassabis D, Kumaran D, Vann SD, Maguire EA. Patients with hippocampal amnesia cannot imagine new experiences. Proc. Natl. Acad. Sci. U. S. A. 2007; 104:1726–1731. [PubMed: 17229836]

Huang H, Zhang J, Wakana S, Zhang W, Ren T, Richards LJ, Yarowsky P, Donohue P, Graham E, van Zijl PC, Mori S. White and gray matter development in human fetal, newborn and pediatric brains. NeuroImage. 2006; 33:27–38. [PubMed: 16905335]

Huang H, Xue R, Zhang J, Ren T, Richards LJ, Yarowsky P, Miller MI, Mori S. Anatomical characterization of human fetal brain development with diffusion tensor magnetic resonance imaging. J. Neurosci. 2009; 29:4263–4273. [PubMed: 19339620]

Humphrey T. The development of the human hippocampal fissure. J. Anat. 1967; 101:655. [PubMed: 6059818]

Ibarretxe-Bilbao N, Ramirez-Ruiz B, Tolosa E, Marti MJ, Valldeoriola F, Bargallo N, Junque C. Hippocampal head atrophy predominance in Parkinson's disease with hallucinations and with dementia. J. Neurol. 2008; 255:1324–1331. [PubMed: 18821043]

Insausti R, Cebada-Sánchez S, Marcos P. Postnatal development of the human hippocampal formation. Adv. Anat. Embryol. Cell Biol. 2010; 206:1. [PubMed: 20329667]

Jacob FD, Habas PA, Kim K, Corbett-Detig J, Xu D, Studholme C, Glenn OA. Fetal hippocampal development: analysis by magnetic resonance imaging volumetry. Pediatr. Res. 2011; 69:425–429. [PubMed: 21270675]

Joseph J, Warton C, Jacobson SW, Jacobson JL, Molteno CD, Eicher A, Marais P, Phillips OR, Narr KL, Meintjes EM. Three-dimensional surface deformation-based shape analysis of hippocampus and caudate nucleus in children with fetal alcohol spectrum disorders. Hum. Brain Mapp. 2014; 35:659–672. [PubMed: 23124690]

Kier EL, Fulbright RK, Bronen RA. Limbic lobe embryology and anatomy: dissection and MR of the medial surface of the fetal cerebral hemisphere. AJNR Am. J. Neuroradiol. 1995; 16:1847–1853. [PubMed: 8693985]

Kier EL, Kim JH, Fulbright RK, Bronen RA. Embryology of the human fetal hippocampus: MR imaging, anatomy, and histology. AJNR Am. J. Neuroradiol. 1997; 18:525–532. [PubMed: 9090416]

Lin X, Zhang Z, Teng G, Meng H, Yu T, Hou Z, Fang F, Zang F, Liu S. Measurements using 7.0 T post-mortem magnetic resonance imaging of the scalar dimensions of the fetal brain between 12 and 20 weeks gestational age. Int. J. Dev. Neurosci. 2011; 29:885–889. [PubMed: 21820045]

Malykhin NV, Bouchard TP, Ogilvie CJ, Coupland NJ, Seres P, Camicioli R. Three-dimensional volumetric analysis and reconstruction of amygdala and hippocampal head, body and tail. Psychiatry Res. 2007; 155:155–165. [PubMed: 17493789]

Meng H, Zhang Z, Geng H, Lin X, Feng L, Teng G, Fang F, Zang F, Liu S. Development of the subcortical brain structures in the second trimester: assessment with 7.0-T MRI. Neuroradiology. 2012; 54:1153–1159. [PubMed: 22811291]

Miranda RC. MicroRNAs and fetal brain development: implications for ethanol teratology during the second trimester period of neurogenesis. Front. Genet. 2012; 3:77. [PubMed: 22623924]

Moser MB, Moser EI. Functional differentiation in the hippocampus. Hippocampus. 1998; 8:608–619. [PubMed: 9882018]

Müller F, O'Rahilly R. Occipitocervical segmentation in staged human embryos. J. Anat. 1994; 185:251. [PubMed: 7961131]

Naidich TP, Daniels D, Haughton V, Pech P, Williams A, Pojunas K, Palacios E. Hippocampal formation and related structures of the limbic lobe: anatomic-MR correlation. Part II. Sagittal sections. Radiology. 1987a; 162:755–761. [PubMed: 3809490]

Naidich TP, Daniels D, Haughton V, Williams A, Pojunas K, Palacios E. Hippocampal formation and related structures of the limbic lobe: anatomic-MR correlation. Part I. Surface features and coronal sections. Radiology. 1987b; 162:747–754. [PubMed: 3809489]

Patrick MJ. Influence of maternal renal infection on the foetus and infant. Arch. Dis. Child. 1967; 42:208. [PubMed: 6024471]

Pfluger T, Weil S, Weis S, Vollmar C, Heiss D, Egger J, Scheck R, Hahn K. Normative volumetric data of the developing hippocampus in children based on magnetic resonance imaging. Epilepsia. 1999; 40:414–423. [PubMed: 10219266]

Prayer D, Kasprian G, Krampl E, Ulm B, Witzani L, Prayer L, Brugger PC. MRI of normal fetal brain development. Eur. J. Radiol. 2006; 57:199–216. [PubMed: 16413984]

Pruessner JC, Li LM, Serles W, Pruessner M, Collins DL, Kabani N, Lupien S, Evans AC. Volumetry of hippocampus and amygdala with high-resolution MRI and three-dimensional analysis software: minimizing the discrepancies between laboratories. Cereb. Cortex. 2000; 10:433–442. [PubMed: 10769253]

Rakic P, Yakovlev PI. Development of the corpus callosum and cavum septi in man. J. Comp. Neurol. 1968; 132:45–72. [PubMed: 5293999]

Sandlin AT, Chauhan SP, Magann EF. Clinical relevance of sonographically estimated amniotic fluid volume polyhydramnios. J. Ultrasound Med. 2013; 32:851–863. [PubMed: 23620328]

Schobel SA, Lewandowski NM, Corcoran CM, Moore H, Brown T, Malaspina D, Small SA. Differential targeting of the CA1 subfield of the hippocampal formation by schizophrenia and related psychotic disorders. Arch. Gen. Psychiatry. 2009; 66:938–946. [PubMed: 19736350]

Shi Y, Morra JH, Thompson PM, Toga AW. Inverse-consistent surface mapping with Laplace–Beltrami eigen-features. Information Processing in Medical Imaging: Proceedings of the Conference. 2009; 21:467–478. [PubMed: 19694286]

Shi Y, Lai R, Morra JH, Dinov I, Thompson PM, Toga AW. Robust surface reconstruction via Laplace–Beltrami eigen-projection and boundary deformation. IEEE Trans. Med. Imaging. 2010; 29:2009–2022. [PubMed: 20624704]

Shi Y, Lai R, Wang DJ, Pelletier D, Mohr D, Sicotte N, Toga AW. Metric optimization for surface analysis in the Laplace–Beltrami embedding space. IEEE Trans. Med. Imaging. 2014; 33:1447–1463.

Sizonenko SV, Borradori-Tolsa C, Bauthay DM, Lodygensky G, Lazeyras F, Huppi P. Impact of intrauterine growth restriction and glucocorticoids on brain development: insights using advanced magnetic resonance imaging. Mol. Cell. Endocrinol. 2006; 254–255:163–171.

Stan AD, Ghose S, Gao X-M, Roberts RC, Lewis-Amezcua K, Hatanpaa KJ, Tamminga CA. Human postmortem tissue: what quality markers matter? Brain Res. 2006; 1123:1–11. [PubMed: 17045977]

Tae WS, Kim SS, Lee KU, Nam EC, Choi JW, Park JI. Hippocampal shape deformation in female patients with unremitting major depressive disorder. AJNR Am. J. Neuroradiol. 2011; 32:671–676. [PubMed: 21372170]

Takahashi E, Dai G, Rosen GD, Wang R, Ohki K, Folkerth RD, Galaburda AM, Wedeen VJ, Grant PE. Developing neocortex organization and connectivity in cats revealed by direct correlation of diffusion tractography and histology. Cereb. Cortex. 2011; 21:200–211. [PubMed: 20494968]

Thompson PM, Hayashi KM, De Zubicaray GI, Janke AL, Rose SE, Semple J, Hong MS, Herman DH, Gravano D, Doddrell DM, Toga AW. Mapping hippocampal and ventricular change in Alzheimer disease. NeuroImage. 2004; 22:1754–1766. [PubMed: 15275931]

Thompson DK, Wood SJ, Doyle LW, Warfield SK, Lodygensky GA, Anderson PJ, Egan GF, Inder TE. Neonate hippocampal volumes: prematurity, perinatal predictors, and 2-year outcome. Ann. Neurol. 2008; 63:642–651. [PubMed: 18384167]

Thompson DK, Wood SJ, Doyle LW, Warfield SK, Egan GF, Inder TE. MR-determined hippocampal asymmetry in full-term and preterm neonates. Hippocampus. 2009; 19:118–123. [PubMed: 18767066]

Torkildsen A. The gross anatomy of the lateral ventricles. J. Anat. 1934; 68:480. [PubMed: 17104497]

Türtscher H, Raio L, Lüscher K, Binswanger R, Brühwiler H. Medically indicated termination of pregnancy in giant uterinemyoma andmono-amniotic twin pregnancy: a case report. Schweiz. Med. Wochenschr. 1999; 129:772–775. [PubMed: 10413811]

Utsunomiya H, Takano K, Okazaki M, Mitsudome A. Development of the temporal lobe in infants and children: analysis by MR-based volumetry. AJNR Am. J. Neuroradiol. 1999; 20:717–723. [PubMed: 10319988]

Villar J, Bergsjg P. Scientific basis for the content of routine antenatal care I. Philosophy, recent studies, and power to eliminate or alleviate adverse maternal outcomes. Acta Obstet. Gynecol. Scand. 1997; 76:1–14. [PubMed: 9033238]

Waldorf KMA, McAdams RM. Influence of infection during pregnancy on fetal development. Reproduction. 2013; 146:R151–R162. [PubMed: 23884862]

Watson C, Andermann F, Gloor P, Jones-Gotman M, Peters T, Evans A, Olivier A, Melanson D, Leroux G. Anatomic basis of amygdaloid and hippocampal volume measurement by magnetic resonance imaging. Neurology. 1992; 42:1743–1750. [PubMed: 1513464]

Winterburn JL, Pruessner JC, Chavez S, Schira MM, Lobaugh NJ, Voineskos AN, Chakravarty MM. A novel in vivo atlas of human hippocampal subfields using high-resolution 3 T magnetic resonance imaging. NeuroImage. 2013; 74:254–265. [PubMed: 23415948]

Wright IC, McGuire PK, Poline JB, Travere JM, Murray RM, Frith CD, Frackowiak RS, Friston KJ. A voxel-based method for the statistical analysis of gray and white matter density applied to schizophrenia. NeuroImage. 1995; 2:244–252. [PubMed: 9343609]

Yanike M, Wirth S, Suzuki WA. Representation of well-learned information in the monkey hippocampus. Neuron. 2004; 42:477–487. [PubMed: 15134643]

Yushkevich PA, Avants BB, Pluta J, Das S, Minkoff D, Mechanic-Hamilton D, Glynn S, Pickup S, Liu W, Gee JC, Grossman M, Detre JA. A high-resolution computational atlas of the human hippocampus from postmortem magnetic resonance imaging at 9.4 T. NeuroImage. 2009; 44:385–398. [PubMed: 18840532]

Zaidel DW. The case for a relationship between human memory, hippocampus and corpus callosum. Biol. Res. 1995; 28:51–57. [PubMed: 8728820]

Zhan J, Dinov ID, Li J, Zhang Z, Hobel S, Shi Y, Lin X, Zamanyan A, Feng L, Teng G, Fang F, Tang Y, Zang F, Toga AW, Liu S. Spatial–temporal atlas of human fetal brain development during the early second trimester. NeuroImage. 2013; 82:115–126. [PubMed: 23727529]

Zhang Z, Liu S, Lin X, Sun B, Yu T, Geng H. Development of fetal cerebral cortex: assessment of the folding conditions with post-mortem magnetic resonance imaging. Int. J. Dev. Neurosci. 2010; 28:537–543. [PubMed: 20457247]

Zhang Z, Liu S, Lin X, Teng G, Yu T, Fang F, Zang F. Development of fetal brain of 20 weeks gestational age: assessment with post-mortem Magnetic Resonance Imaging. Eur. J. Radiol. 2011; 80:e432–e439. [PubMed: 21146341]

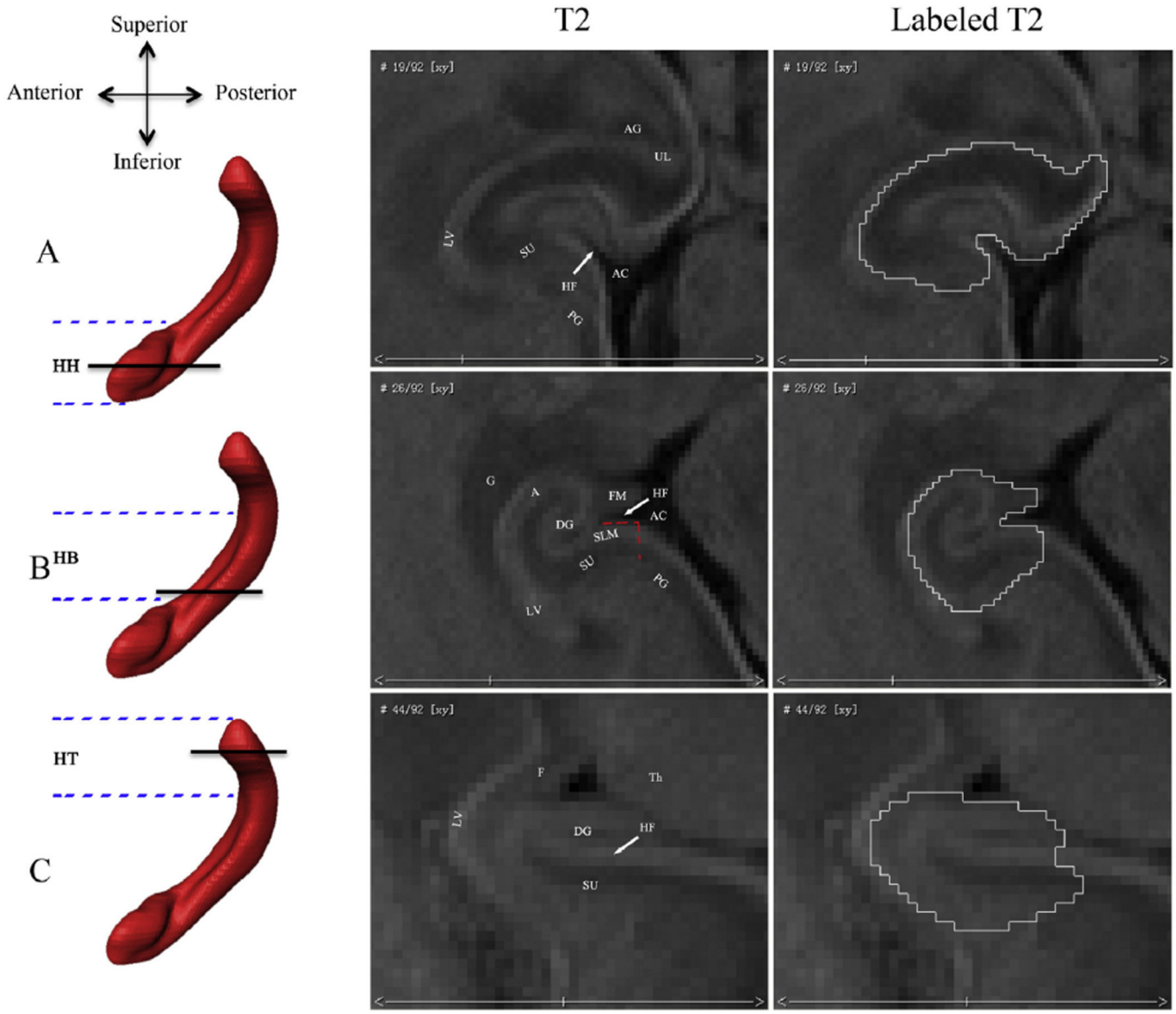

Fig. 1.

Borders of the fetal hippocampal formation in the axial plane. The rows show different axial levels of the hippocampal formation (HF): (A) hippocampal head (HH); (B) hippocampal body (HB); and (C) hippocampal tail (HT). The parallel black lines on the left 3D sagittal hippocampal renderings indicate where the corresponding axial slices are along the inferior–superior axis. The parallel blue imaginary lines indicate the approximate ranges of the HH, HB, and HT. The right two columns of T2 images show the axial view of the fetal hippocampal formation and its segmentations. Abbreviations show different brain structures: (AC) ambient cistern; (UL) uncal recess of the temporal horn of the lateral ventricle; (LV) lateral ventricle; (PG) parahippocampal gyrus; (HF) hippocampal fissure; (G) germinalmatrix; (F) fornix; (FM) fimbria; (SU) subiculum; (SLM) superficial medullary lamina; (Th) thalamus; (DG) dentate gyrus; (A) alveus; and (AG) amygdala.

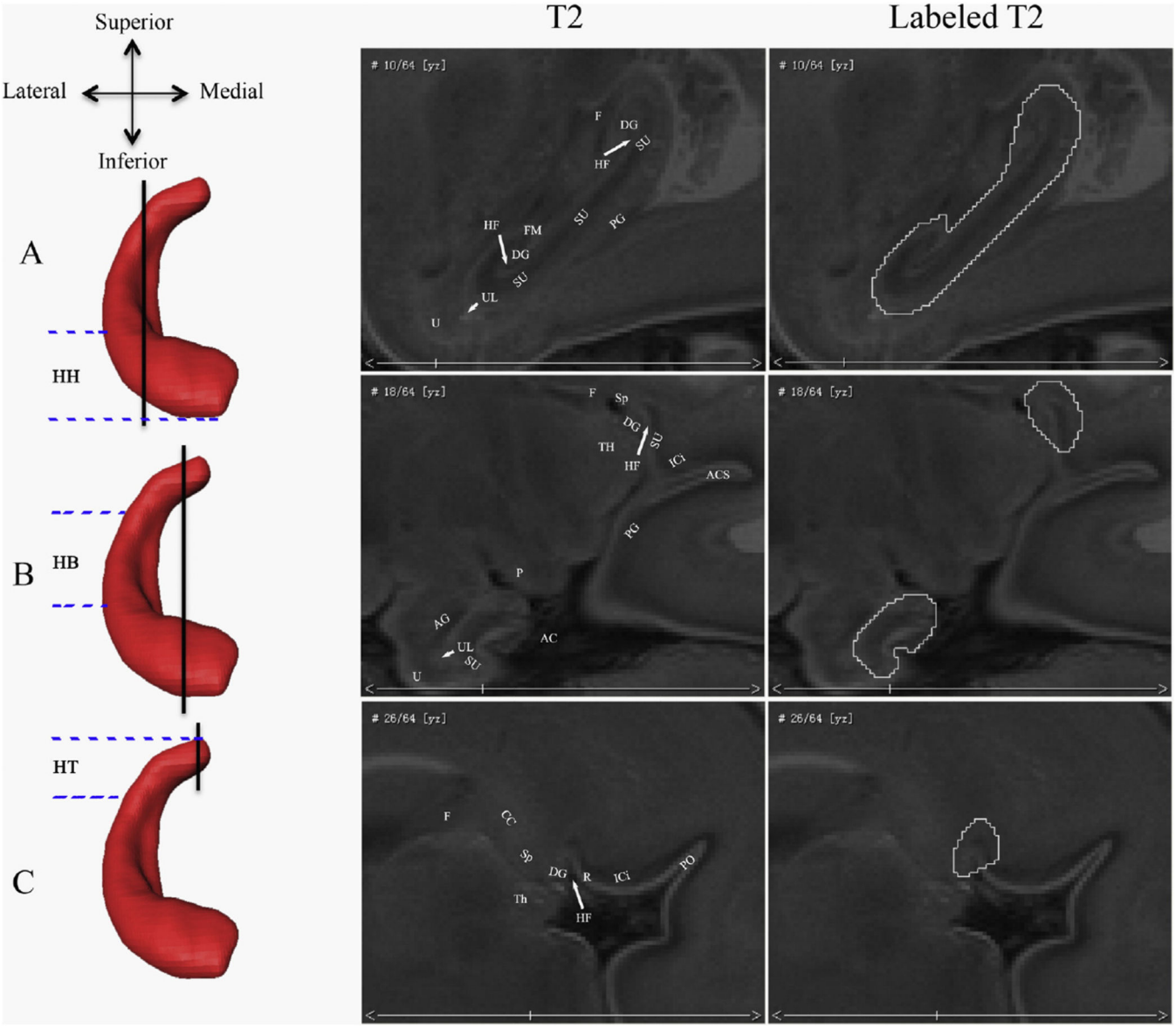

Fig. 2.

Borders of the fetal hippocampal formation in the sagittal plane. The rows show different sagittal levels of the hippocampal formation (HF). The vertical black lines on the left 3D coronal hippocampal renderings indicate where the corresponding sagittal slices are along the lateral–medial axis. The parallel blue imaginary lines indicate the approximate ranges of the HH, HB, and HT. The right two columns of T2 images show the sagittal view of the fetal hippocampal formation and its segmentations. Abbreviations show different brain structures: (AC) ambient cistern; (UL) uncal recess of the temporal horn of the lateral ventricle; (ICi) isthmus of the cingulate gyrus; (PG) parahippocampal gyrus; (HF) hippocampal fissure; (Sp) splenium of the corpus callosum; (F) fornix; (R) retrosplenial cortex; (FM) fimbria; (SU) subiculum; (P) cerebral peduncle; (Th) thalamus; (DG) dentate gyrus; (AG) amgydala; (CC) corpus callosum; (ACS) anterior calcarine sulcus; (PO) parietooccipital sulcus; and (U) uncus.

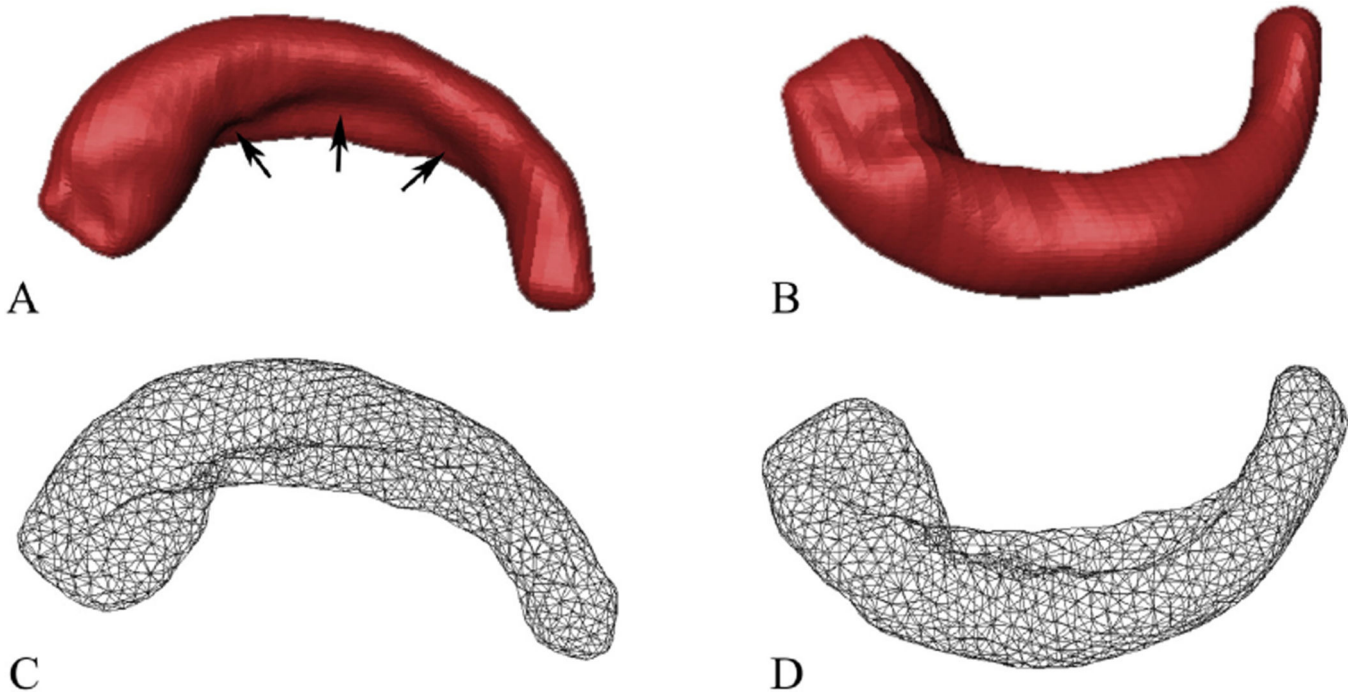

Fig. 3.

Superior (left) and inferior (right) views of one 3D model of the right HF and its corresponding surface meshes. (A and B) The 3D representation models reconstructed from the segmented masks. (C and D) The corresponding mesh representations. The black arrows in A show the hippocampal fissure.

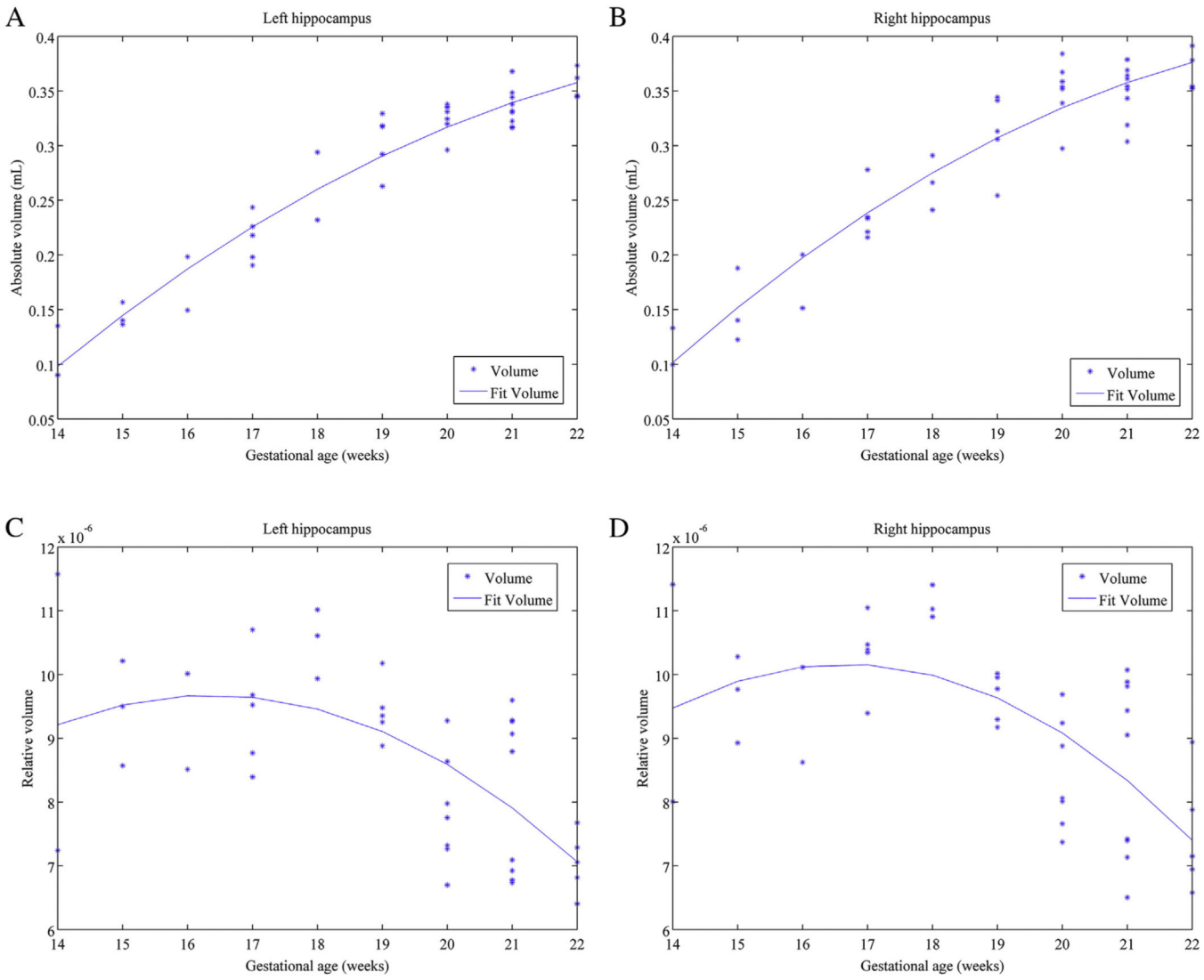

Fig. 4.

Scatterplots and tendencies between the left and right hippocampal absolute and relative volumes and gestational age in weeks. (A) Tendency of the absolute left hippocampal volume. (B) Tendency of the absolute right hippocampal volume. (C) Tendency of the relative left hippocampal volume. (D) Tendency of the relative right hippocampal volume.

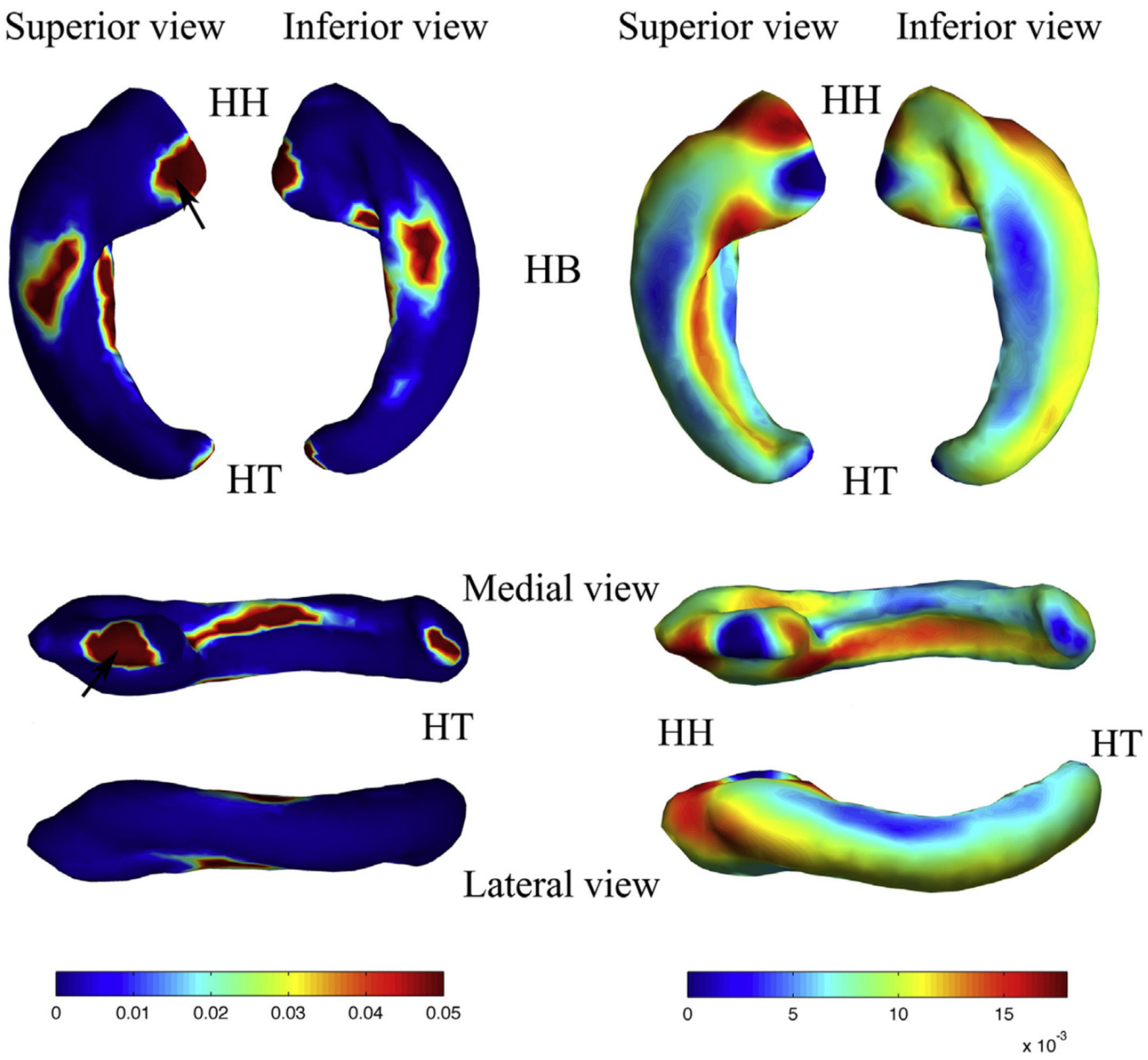

Fig. 5.

p value map (left) and regression coefficient map (right) of the shape statistics of the left HF. Superior, inferior, medial, and lateral views are shown, respectively. Abbreviations: (HH) hippocampal head; (HB) hippocampal body; (HT) hippocampal tail. The black arrows in the p value map indicate the regions adjacent to amygdala.

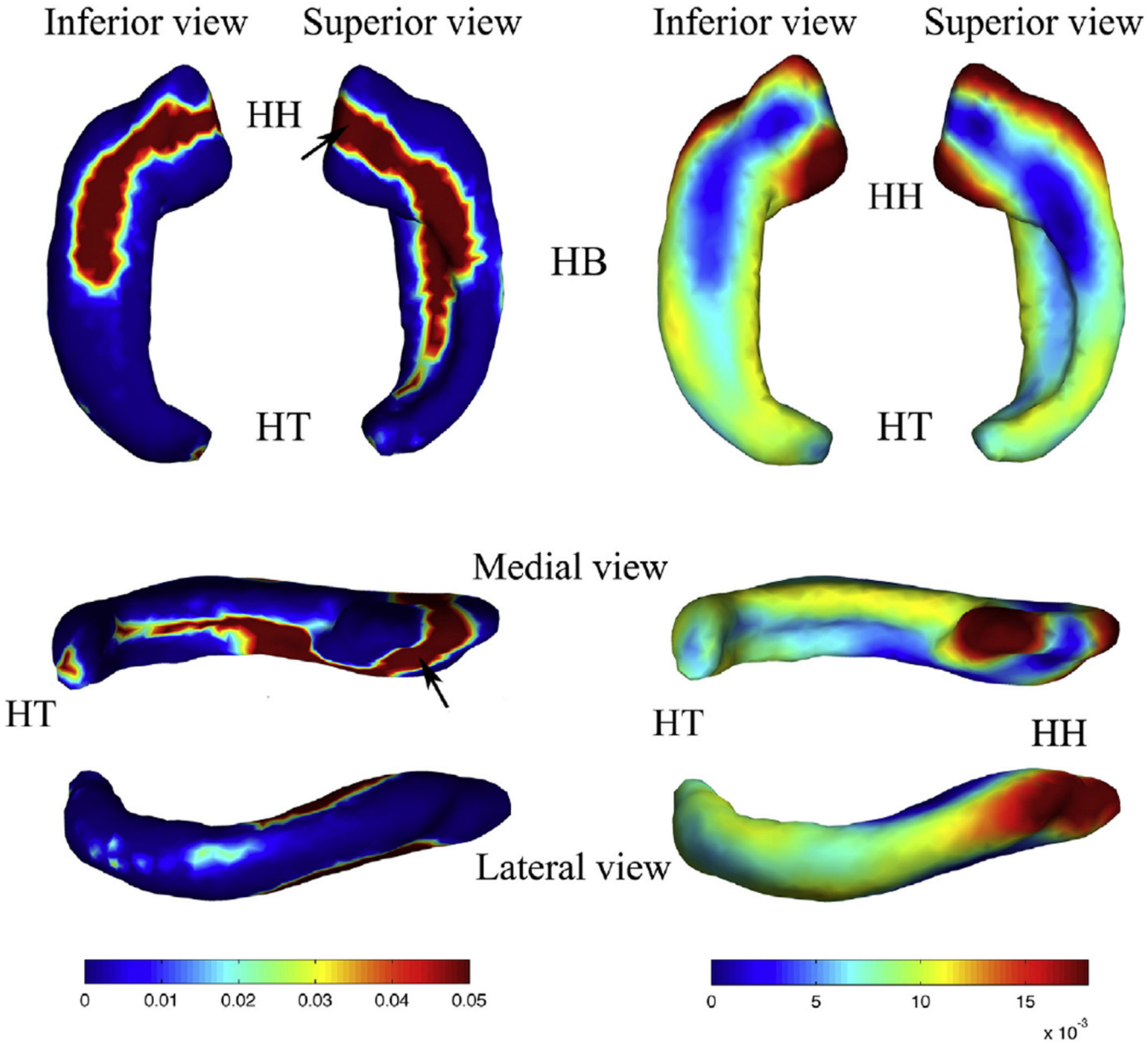

Fig. 6.

p value map (left) and regression coefficient map (right) of the shape statistics of the right HF. Inferior, superior, medial, and lateral views are shown, respectively. Abbreviations: (HH) hippocampal head; (HB) hippocampal body; (HT) hippocampal tail. The black arrows in the p value map indicate the regions adjacent to amygdala.

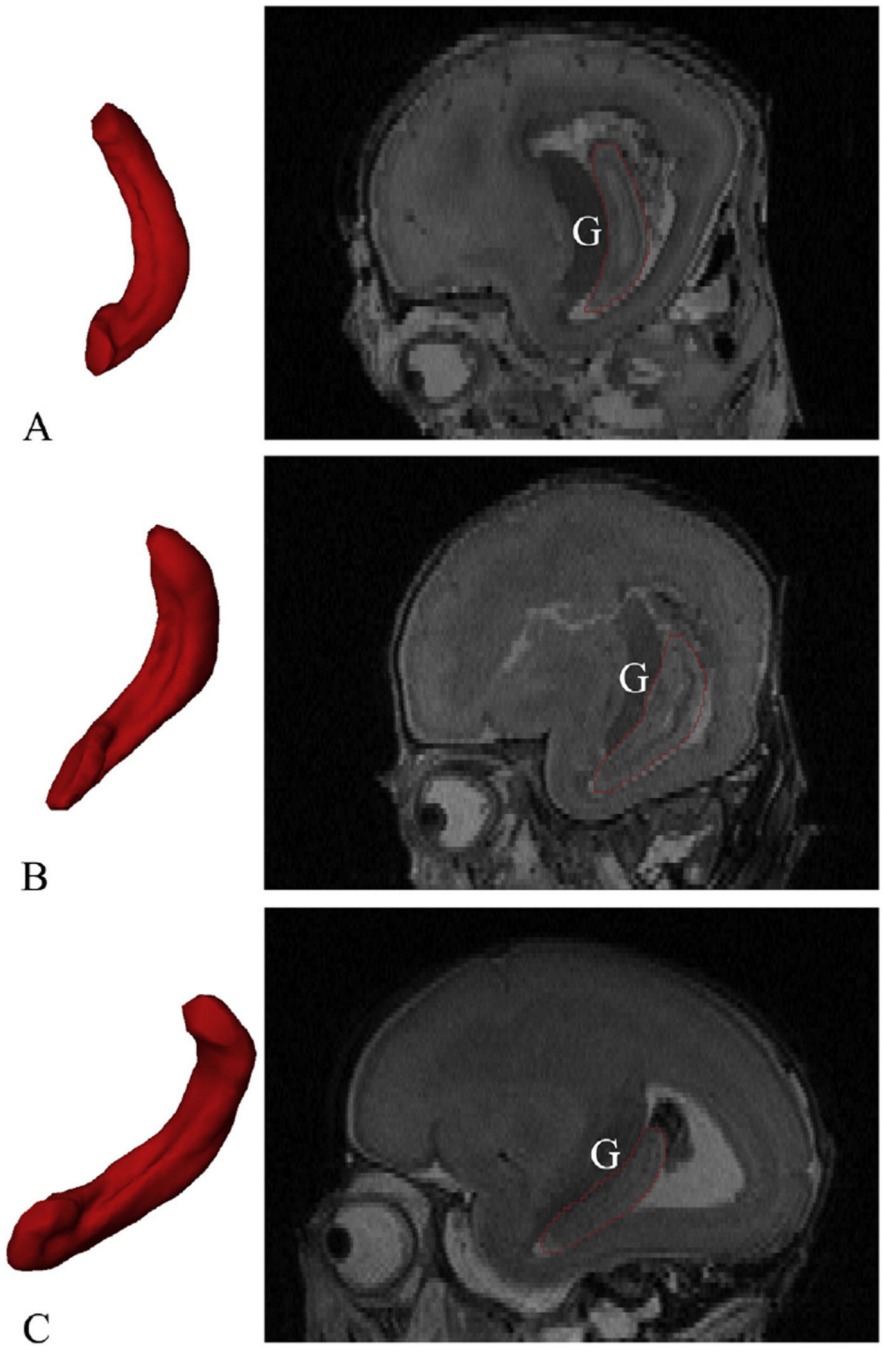

Fig. 7.

Positioning changes of the fetal HF. The left 3Dmodels are the 3D representations of the right HF reconstructed from the segmented masks (medial view, relative volume), and the right sections are the same sagittal section passes through the germinal matrix (G). The whole HF is becoming horizontal as its head folding into the temporal lobe. From top to bottom: (A) 15 GW; (B) 18 GW; and (C) 21 GW.

Table 1

The demographic information of the specimens.

Gestational age (week)	Number (total of 41)	Termination of pregnancy	Gender (male/female)
14	2	SA (2)	1/1
15	3	SA (2), TI	1/2
16	2	SA, SIC	2/0
17	5	SA (2), SIC, TI, UNK	1/4
18	3	SA, TI, UNK	3/0
19	5	SA (2), SIC (2), FCA	2/3
20	7	SA (3), SIC (2), FCA, UNK	1/6
21	9	SA (4), SIC (3), FCA, UNK	1/8
22	5	FCA, SIC (2), UNK (2)	1/4

Abbreviations: (FCA) fetal chromosomal abnormality; (TI) teratogenesis infection; (SA) spontaneous abortion; (SIC) stressful intrauterine conditions; (UNK) unknown reasons of malformation (not brain) detected by MRI.